arXiv:1209.3097v1 [cond-mat.str-el] 14 Sep 2012

# Gapless edge states and their stability in two-dimensional quantum magnets

Takafumi Suzuki[1] and Masahiro Sato[2]
[1]Research Center for Nano-Micro Structure Science and Engineering,
Graduate School of Engineering, University of Hyogo, Himeji, Hyogo 671-2280, Japan
[2]Department of Physics and Mathematics, Aoyama Gakuin University, Sagamihara, Kanagawa 229-8558, Japan

(Dated: September 17, 2012)

We study the nature of edge states in extrinsically and spontaneously dimerized states of two-dimensional spin-$\frac{1}{2}$ antiferromagnets, by performing quantum Monte Carlo simulation. We show that a gapless edge mode emerges in the wide region of the dimerized phases, and the critical exponent of spin correlators along the edge deviates from the value of Tomonaga-Luttinger liquid (TLL) universality. We also demonstrate that the gapless nature at edges is stable against several perturbations such as external magnetic field, easy-plane XXZ anisotropy, Dzyaloshinskii-Moriya interaction, and further-neighbor exchange interactions. The edge states exhibit non TLL behavior, depending strongly on model parameters and perturbations. Possible ways of detecting these edge states are discussed.

PACS numbers: 75.10.Jm, 75.10.Pq, 75.10.Kt, 73.43.-f, 75.10.-b

*Introduction.*− In recent years, gapful ground states without any *local* order parameter and their boundary properties have been vividly studied in quantum many-body physics from both theoretical and experimental viewpoints. Among such disordered states, for instance, two- and three-dimensional (3D) topological insulators (TIs) have attracted much attention as novel many-body phases in solids.[1,2] Their fundamental properties are that the bulk has a finite excitation gap, but its boundary (surface or edge) is metallic (i.e., gapless) and around the boundary, up-spin electrons move antiparallel to the motion of down-spin electrons (this nature is called helical). This gapless boundary state is quite stable against any perturbation with time reversal symmetry, and the existence of a helical edge mode is recorded in a $\mathbb{Z}_2$ topological invariant defined on the bulk (bulk-edge correspondence).

In quantum spin systems, the Haldane-gap state[3] is also famous as a state without any local order. This state is defined as the ground state of 1D spin-1 antiferromagnetic (AF) chains and is actually realized in some quasi-1D magnets.[4,5] Its characteristic features can be captured by valence-bond solid (VBS) picture.[6] Namely, the Haldane state can be approximated by the uniform tensor product state of local singlet dimers comprised from two fictitious $S = \frac{1}{2}$ spins on neighboring sites, which are generated via the decomposition of original $S = 1$ spin on each site. From the solid singlet distribution, we can easily understand the existence of a finite excitation gap (called Haldane gap) on the Haldane state. Similarly, the uniform alignment of singlets indicates the absence of any local order parameter, but we can construct a *non-local* string order parameter[7] to distinguish the Haldane state from the other paramagnetic phases. The VBS picture also shows that an almost free $S = \frac{1}{2}$ spin appears at the edge of finite-size spin-1 Haldane state under free boundary condition.[5] In addition to these results, recently new ways of characterizing the Haldane states have been actively discussed based on symmetries and artificial quantities such as entanglement spectra.[8–10]

All of the gapped, topological phases in free fermion systems including TI have been succeeded in being classified theoretically.[11–13] On the other hand, topological phases and boundary states in quantum spin systems have been less understood, expect for a few VBS (such as the Haldane state) and short-range valence-bond states in 1D spin systems including spin ladders. Therefore, the understanding of topological nature and boundary properties in quantum spin systems, especially, in *higher-dimensional* magnets, is an important, fundamental issue in magnetism. One might image VBS[14] or exotic spin-liquid states as typical examples of 2D or 3D gapped non-magnetic spin states with a gapless edge mode. It is however difficult to prepare such states in nature because the corresponding Hamiltonians contain various tuned coupling constants. Simple, realistic systems with a gapless edge mode would be suitable for starting to understand edge modes in 2D and 3D spin systems. In this paper, we thus study the nature of edge modes in 2D spin-Peierls (dimerized) states, by using quantum Mote Carlo (QMC) simulation based on the worm algorithm.[15–17]

There is a similarity between TI and the Haldane state; A finite bulk gap, gapless boundary states, and $\mathbb{Z}_2$ topological invariant of TI seem to correspond to a Haldane gap, free edge spins, and the string order parameter of the Haldane state, respectively. We will hence consider how the edge modes of dimerized states are different from/similar to those of TIs and the Haldane state. It would be impossible to define any topological order parameter for 2D dimerized states, and in that sense, the gapless edge states in dimerized states (even if exist) are naively expected to be less stable compared to those of TIs. We should however note that it is generally hard to predict whether or not there exist gapless edge states and how stable they are, since quantum spin systems we consider below are strongly correlated systems differently from free fermion models for TIs.

*Model.*− Dimerized phases are roughly classified into

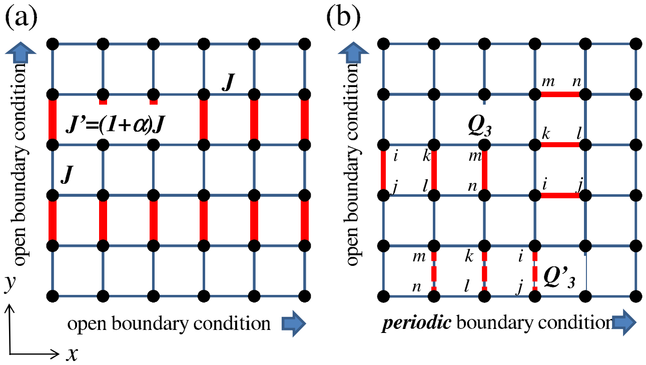

FIG. 1: (color online) (a) 2D dimerized model with bond alternation along the $y$ direction. (b) 2D $JQ_3$ model with six-spin interaction term. The modified coupling constant $Q_3'$ on edges is explained in the text.

an extrinsically dimerized phase without any SSB and an intrinsically dimerized one with a spontaneous translational symmetry breaking. To study those two states we utilize two SU(2)-symmetric spin-$\frac{1}{2}$ AF models on square lattice with size $L \times L$: The dimerized model[18,19] and the $JQ_3$ model.[20] Their Hamiltonians are given as

$$\mathcal{H}_{\rm dim} = \sum_{\langle i,j \rangle} J \boldsymbol{S}_i \cdot \boldsymbol{S}_j + \sum_{j} J\alpha \delta_{j_y,{\rm even}} \boldsymbol{S}_j \cdot \boldsymbol{S}_{j+\boldsymbol{e}_y}, \quad \text{(1a)}$$

$$\mathcal{H}_{JQ3} = \sum_{\langle i,j \rangle} J \boldsymbol{S}_i \cdot \boldsymbol{S}_j + \sum_{\langle i,j,k,l,m,n \rangle} Q_3 C_{ij} C_{kl} C_{mn} \quad \text{(1b)}$$

where $\boldsymbol{S}_j$ is the spin-$\frac{1}{2}$ operator on site $j = (j_x, j_y)$ ($j_{x,y} \in \mathbb{Z}$), $\boldsymbol{e}_{x[y]} = (1,0)$ $[(0,1)]$ is the unit vector for the $x[y]$ direction, $J > 0$ is the AF exchange coupling constant between neighboring spins, and $C_{ij} = 1/4 - \boldsymbol{S}_i \cdot \boldsymbol{S}_j$. In the dimerized model (1a), $\alpha$ denotes the magnitude of external dimerization along the $y$ direction as shown in Fig. 1, in which the dimerized bond strength $J' = J(1+\alpha)$. If $\alpha$ is strong enough and the open boundary condition for $y$ direction is imposed as in Fig. 1, an effective spin chain is expected to appear along the $x$ direction at the edge thanks to the formation of dimerization on every strong bonds $J'$. In the $JQ_3$ model (1b), the second $Q_3$ term includes six-spin interactions, where six sites $(i,j,k,l,m,n)$ are defined by two neighboring plaquettes (rectangle) shown in Fig. 1. The symbol $\sum_{\langle i,j,k,l,m,n \rangle}$ stands for the summation over all rectangles on square lattice.

The ground-state phase diagrams for the dimerized and $JQ_3$ models have been investigated by QMC calculations, and both models show the Néel-dimer quantum phase transition.[21] For the dimerized model, the critical point is located at $J' = J'_c \simeq 1.91J$[18,19] and singlet dimers appear on all the bonds $J'$ for $J' > J'_c$. The transition of the $JQ_3$ model takes place at $Q_3 = Q_{3c} \simeq 1.5J$ and the spins spontaneously form a columnar dimer state along the $x$ or $y$ direction when $Q_3 > Q_{3c}$.[20] It is worth notice that the dimer phase of Eq. (1a) does not accompany any SSB similarly to TI, while in the case of Eq. (1b), the translational symmetry is spontaneously broken.

The $JQ_3$ model seems to be a toy model, but it is one of the few spin models with a spontaneously dimerized phase and can be accurately analyzed by QMC simulation without negative sign problem. Furthermore, its dimerized ground-state wave function is expected to be close enough to that of real dimerized magnets. To study possible gapless edge modes of the model (1a), we impose open boundary condition for the $y$ direction as shown in Fig. 1. We have confirmed from the QMC simulation that in the dimer phase of the $JQ_3$ model, singlet dimers tend to reside on the edge. For this dimerization pattern, no gapless edge state is expected. In order to remove the dimers on edges and make the same dimerization pattern as that of the dimerized model (1a), we modify the value of $Q_3$ to $Q_3'(< Q_3)$ at the edge as depicted in Fig. 1. From QMC results of $Q_3'/Q_3 = 0, 0.25$, and $0.5$, we have checked that the resultant dimers do not reside on the edges and the nature of edge states is not sensitive for changing the value of $Q_3'$. We therefore set $Q_3'/Q_3 = 0.5$ throughout this paper.

*1D liquid.–* In order to judge whether or not a gapless edge mode are present, we utilize two-point spin correlation functions at edge of two models in Eq. (1). If it exists, an algebraic decay of the correlators is expected, while the correlators decay in an exponential fashion when the edge state has a finite excitation gap. When the dimerized model approaches to the limit $\alpha \to \infty$, an isolated spin-$\frac{1}{2}$ AF chain appears at the edge and its low-energy physics is governed by a gapless Tomonaga-Luttinger (TL) liquid. It is therefore important to summarize spin corrrelators of the TL-liquid phase as a reference point before embarking on our QMC results. For an ideal TL liquid phase of spin-$\frac{1}{2}$ AF chains, spin correlations are known to behave as[22]

$$\langle S_r^x S_0^x \rangle \sim C_1 (-1)^r r^{-\eta_{xy}} + \cdots, \quad \text{(2a)}$$

$$\langle S_r^z S_0^z \rangle \sim m^2 + C_2 r^{-\eta_z} \cos(2k_F r) + \cdots, \quad \text{(2b)}$$

at long distances $r \gg 1$. Here the magnetization $m = \langle S_j^z \rangle$ is induced by external uniform field $H$, $2k_F = \pi(1-2m)$ is the "Fermi" wave number, and $C_{1,2}$ are non-universal constants. It is well known that critical exponents $\eta_{xy,z}$ satisfy the relation $\eta_{xy}\eta_z = 1$,[22] and $\eta_{xy} = \eta_z = 1$ occurs at the SU(2)-symmetric case. We also note that a $2k_F$ incommesurate oscillation disappears at $m = H = 0$ in Eq. (2b).

*Numerical analysis.–* Now we discuss the QMC results of two models (1a) and (1b). Figure 2 shows numerically determined spin correlation functions along the $x$ direction on edge and those along the $y$ direction at $x = L/2$ for the dimerized phases of both dimerized and $JQ_3$ models at a sufficiently low temperature $T$. Hereafter, a correlation function along the $x$ direction on edge (along the $y$ direction) is called edge (bulk) correlation. The long-distance behavior of edge spin correlations $S_{\mu\mu}(r_x) \equiv \langle S^\mu_{(r_x,0)} S^\mu_{(0,0)} \rangle$ are well explained by a power-law decay in both models, reflecting the existence of a gapless edge state. The critical exponents $\eta$ defined by $|S_{\mu\mu}(r)| \sim r^{-\eta}$ is evaluated as $\eta \simeq 1.13$ (0.97) for the dimer ($JQ_3$) model. We stress that *this algebraic-decay behavior survives far from the dimer limit.* In fact, the parameters $Q_3/J = 2.5$ and $J'/J = 2$ correspond to $Q_3/Q_{3_c} \simeq 1.67$ and $J'/J'_c \simeq 1.05$, respectively. Furthermore, the critical exponent $\eta$ somewhat violates a TL-liquid relation $\eta_{xy} = \eta_z = 1$. This implies the two dimensionality affects the gapless edge state. We have also evaluated $\eta \simeq 1.01$ (0.99) at a deeper dimerized point $J'/J = 5$ ($Q_3/J = 4$) in the dimerized ($JQ_3$) model. On the other hand, as shown in the inset of Fig. 2, the bulk spin correlations $B_{\mu\mu}(r_y) \equiv \langle S^{\mu}_{(L/2,r_y)} S^{\mu}_{(L/2,0)} \rangle$ decay exponentially, indicating a finite dimerization gap in the bulk. The correlation lengths $\xi_y$ of $|B_{\mu\mu}(r_y)| \sim \exp[-r_y/\xi_y]$ are evaluated as $\xi_y \sim 7.4$ (4.0) for the dimerized ($JQ_3$) model. These large values of $\xi_y$ clearly show that the edge chain is really correlated to the bulk. From these results, we conclude that a gapless edge state is realized in the wide range of both extrinsically and spontaneously spin-Peierls phases, but the exponent deviates from that of TL liquid, especially, near the 2D critical points.

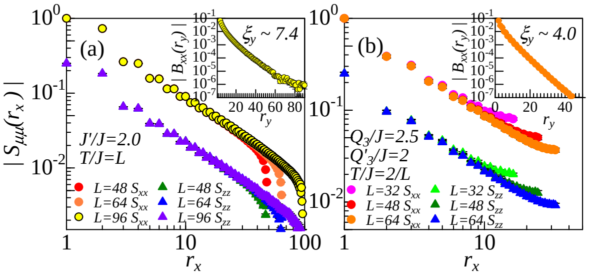

FIG. 2: (color online) Spin-spin correlation $|S_{\mu\mu}(r_x)| = |\langle S^{\mu}_{(r_x,0)} S^{\mu}_{(0,0)} \rangle|$ on the edge in the dimerized phase of (a) dimerized model and (b) $JQ_3$ model. Insets are the results along the bulk direction: $|B_{\mu\mu}(r_y)| = |\langle S^{\mu}_{(L/2,r_y)} S^{\mu}_{(L/2,0)} \rangle|$. We normalize the values of $|S_{\mu\mu}(1)|$ and $|B_{\mu\mu}(1)|$ to be unity. We depict only the results for $B_{xx}$ because of the $SU(2)$ symmetry of the models. Errors are drawn on all symbols, but they are less than the symbol size.

*Stability against perturbations.—* We next discuss how robust the gapless edge mode is against various kinds of perturbations. This is very important since the lack of the stability indicates the difficulty of observing the edge state in real magnets. As realistic perturbations, we consider (1) uniform Zeeman term $\mathcal{H}_z = -H\sum_j S^z_j$, (2) XXZ-type magnetic anisotropy $\mathcal{H}_{\rm xxz} = -J\Delta \sum_{\langle i,j \rangle} S^z_i S^z_j$, (3) Dzyaloshinskii-Moriya (DM) interaction $\mathcal{H}_{\rm DM} = \sum_{\langle i,j \rangle} \boldsymbol{D}_{ij} \cdot (\boldsymbol{S}_i \times \boldsymbol{S}_j)$ with $\boldsymbol{D}_{ij} \parallel S^z$, (4) next-nearest-neighbor interaction perpendicular to the edge direction $\mathcal{H}_{\rm N.N.N} = \sum_{i_x=j_x, i_y+2=j_y} E \boldsymbol{S}_i \cdot \boldsymbol{S}_j$, and (5) additional bond modulation for the $x$ direction These perturbations possess the following nature of symmetry.

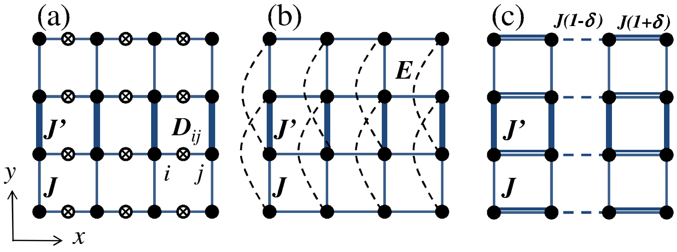

FIG. 3: (color online) Perturbations in the dimerized model: (a) DM interaction, (b) next-nearest neighbor interaction, and (c) bond alternation. Open boundary condition is imposed and the edge state appears parallel to the $x$ direction. Cross circles on $J$ bonds indicate the direction of $\boldsymbol{D}_{i,j}$ vector.

The Zeeman term $\mathcal{H}_z$ breaks time-reversal symmetry, and $\mathcal{H}_{\rm DM}$ does link-parity symmetry. These two and $\mathcal{H}_{\rm xxz}$ reduces the $SU(2)$ symmetry to the axial $U(1)$ type. The bond alternation term $\mathcal{H}_{\rm alt}$ eliminates the translational symmetry along the $x$ direction (if we apply periodic boundary condition). In contrast, $\mathcal{H}_{\rm N.N.N}$ does not violate any symmetry of the original models. They are depicted in Fig. 3.

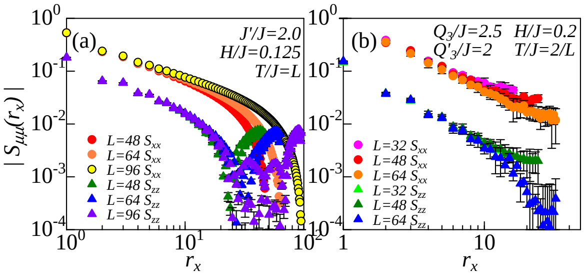

FIG. 4: (color online) Edge spin correlations $S_{\mu\mu}(r_x)$ of (a) dimerized model and (b) $JQ_3$ model under a magnetic field $H$. Circles and triangles are the transverse ($\mu = x$) and longitudinal ($\mu = z$) correlators, respectively. We have eliminated a constant part of $\langle S^z_j \rangle^2$ from the data of $\mu = z$.

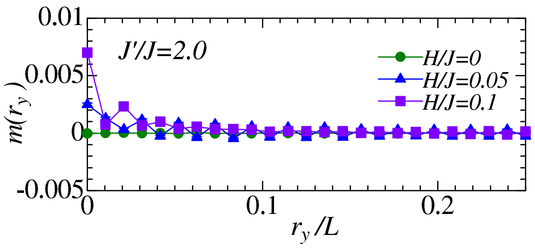

FIG. 5: (color online) Magnetization profile $m(r_y) = \langle S^z_{L/2,r_y} \rangle$ of the dimerized model with $J'/J = 2$ under magnetic fields $H$ at $r_x = L/2$.

First let us consider the effects of the Zeeman term. We plot the edge spin correlations and magnetization profiles in the presence of magnetic field $H$ in Figs. 4 and 5, respectively. Figure 4 shows that even in $H$, a power-low decay fashion survives in the edge spin correlations, having an incommensurate oscillation in the $S^z$ correlation. The stability against $H$ is in contrast to the helical edge of TIs and edge spins of Haldane states. The incommensurability is very similar to Eq. (2b), while such an incommensurate oscillation is absent in the bulk correlations. Figure 5 reveals that a finite magnetization emerges with increase of $H$ *only around the edge*. Finite magnetizations on sites near the edge indicates that some arrays around the edge also become gapless due to a small $H$. This inhomogeneous magnetization profile can be observed in principle, for example, by using nuclear magnetic resonance (NMR). Both Figs. 4 and 5 clearly indicate that the gapless edge mode survives under field $H$.

Next let us consider effects of $\mathcal{H}_{\rm DM}$ and $\mathcal{H}_{\rm xxz}$. For the $JQ_3$ models with perturbations (2)-(5), technical difficulties of the QMC method emerge in high accurate computations. We will therefore focus only on the dimerized model below. However effects of the perturbations on the dimerized model are probably very similar to those on the $JQ_3$ model since the wave functions of both extrinsically and spontaneously dimerized phases are expected to massively overlap each other.

Before the analysis, we should note the following property of the DM interaction. As we consider, for example, a uniform DM term with $\boldsymbol{D}_{ij} = (0, 0, D^z)$, the Hamiltonian $\mathcal{H}_{\rm dim} + \mathcal{H}_{\rm DM}$ can be mapped onto the following easy-plane anisotropic form

$$\begin{aligned}\mathcal{H}' &= \sum_j J_\perp (S^x_j S^x_{j+\boldsymbol{e}_x} + S^y_j S^y_{j+\boldsymbol{e}_x}) + J S^z_j S^z_{j+\boldsymbol{e}_x} \\ &\quad + \sum_j J(1+\alpha\delta_{j_y,\rm even}) \boldsymbol{S}_j \cdot \boldsymbol{S}_{j+\boldsymbol{e}_y}, \qquad (3)\end{aligned}$$

via a proper unitary transformation $S^\pm_r \to e^{i\theta_r} S^\pm_r$.[23,24] Here $J_\perp = J\sqrt{1+(D^z/J)^2}$. Remarkably, the modified system (3) recovers the link-parity symmetry and has an easy-plane anisotropy. This kind of mapping can be applicable for a wide class of DM terms between neighboring spins if we adopt the open boundary condition for both $x$ and $y$ directions. Therefore, it is enough to study the dimerized model with an easy-plane XXZ anisotropy in order to see effects of both $\mathcal{H}_{\rm DM}$ and $\mathcal{H}_{\rm xxz}$.

Figure 6 (a) indicates that both the longitudinal and transverse edge spin correlations decay algebraically in the system (3) with $D^z/J = 0.1$. We thus conclude that the gapless edge state is stable against both the DM and easy-plane XXZ interactions. In purely 1D spin-$\frac{1}{2}$ AF chains with easy-plane anisotropy, critical exponents $\eta_{xy,z}$ usually satisfy $\eta_z > \eta_{xy}$ in addition to $\eta_z\eta_{xy} = 1$.[22] In the present 2D case of Fig. 6 (a), however, we obtain $\eta_{xy} \simeq 0.92$ and $\eta_z \simeq 1.48$. Namely, the exponents satisfy the inequality $\eta_z > \eta_{xy}$, but the relation $\eta_z\eta_{xy} = 1$ is clearly broken down. The difference between critical exponents of the 1D chain and the edge of the 2D dimerized model would be attributed to the correlation between the bulk and edge.

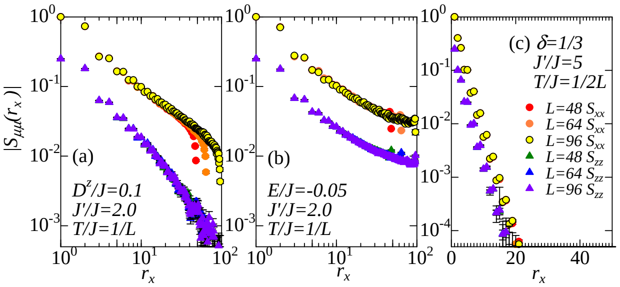

FIG. 6: (color online) Effects of (a) a DM interaction (equal to XXZ anisotropy), (b) a next-nearest neighbor interaction, and (c) an extra bond-alternation along the edge direction on the edge spin correlations of the dimerized model. Circles and triangles are the results of $\mu = x$ and $\mu = z$, respectively. In panel (c), we have used semi-log scale, and have set a larger $J'/J = 5$ and a lower temperature $T = 1/(2L)$ to depict a clear exponential-decay form of the edge correlation.

JQmodel

The edge spin correlations for the case with $\mathcal{H}_{\rm N.N.N}$ are given in Fig. 6 (b), in which we have adopted a ferromagnetic coupling $E/J = -0.05$ to avoid the negative sign problem. The figure shows a power-law decay of the correlation functions, and it indicates that the gapless edge mode still survives in a small $\mathcal{H}_{\rm N.N.N}$. We however note that evaluated critical exponents $\eta_{xy} = \eta_z \sim 0.71$ deviate from the value of ideal TL liquid similarly to the cases with $\mathcal{H}_{\rm DM}$ and $\mathcal{H}_{\rm xxz}$.

Figure 6 (c) is the result of the system $\mathcal{H}_{\rm dim} + \mathcal{H}_{\rm alt}$. As expected, the edge spin correlation changes from an algebraic form to an exponential one due to the bond dimerization along the $x$ direction. From these analyses of perturbations, we see that the gapless nature of the edge state survives after introducing several perturbations with different symmetries except for the bond alternation $\mathcal{H}_{\rm alt}$. It suggests a high possibility of the realization of a gapless edge mode in 2D spin-Peierls phases.

*Experimental ways.*— Finally we discuss possible experimental methods of probing signatures of the gapless edge modes in 2D spin-Peierls states. As we already mentioned, a finite magnetization rapidly grows only around the edge sites as shown in Fig. 5, if we apply $H$ in the dimerized states. Observing such a site-dependent magnetization (e.g., by using NMR) could be a signature of the existence of a gapless edge state. The NMR relaxation rate $1/T_1$ for nuclear spins near the edge is expected to contain a power-law $T$ dependence $T^{-\epsilon}$ at low temperatures,[22] implying the existence of a gapless mode. Inelastic neutron scattering spectra could also provide information about gapless edge modes. In the case of TIs, ARPES spectra have been often used to see the gapless dispersion on the surface/edge in addition to gapped bulk excitations. Similarly, as shown in Fig. 7, the neutron scattering spectra are expected to possess a

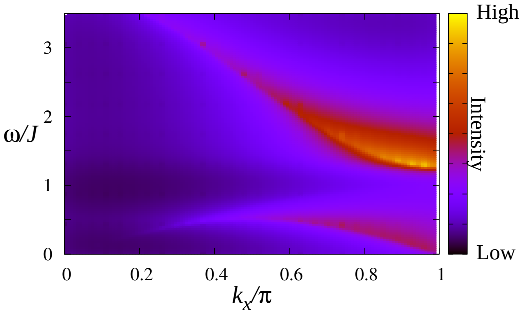

FIG. 7: (color online) Schematic inelastic-neutron-scattering spectrum of a 2D spin-Peierls phase with a gapless edge mode in the space of frequency $\omega$ and the wave number $k_x$. The wave number $k_y$ is fixed to $\pi$. The weight in the low-energy region $\omega/J \lesssim 1$ is the contribution from the edge state, which lower bound would be similar to the des Cloizeaux-Peason mode $\sim J|\sin(k_x)|$. The weight in the higher-energy region comes from the gapped triplet excitations in the bulk.

des Cloizeaux-Peason-like gapless branch[22,25] due to the edge state in 2D Peierls magnets. This would be a strong evidence for the gapless edge mode. In addition to these ways, for instance, heat transport properties would capture the nature of the gapless edge mode.

*Conclusions.–* We have investigated several properties of the edge spins of the dimerized and $JQ_3$ models. When the system is in the dimerized phase and the singlet dimers do not reside on the edge, the gapless edge state really emerges. We have shown that the edge mode is quite robust against various perturbations with different symmetries. Particularly, the stability against external magnetic field $H$ is in contrast with the helical edge modes of TIs and free edge spins of the Haldane state, and $H$ induces an edge magnetization as shown in Fig. 5. The edge spin correlations algebraically decay like a TL liquid, but their critical exponents $\eta_{xy,z}$ generally violate the TL-liquid relation $\eta_{xy}\eta_z = 1$, depending on the detail of the models. NMR, inelastic neutron scattering, and heat transport would be hopeful experimental ways of detecting the gapless edge modes.

We thank J. Lou and H. Tsunetsugu for fruitful discussions. Numerical calculations were performed at the ISSP Supercomputer Center of the University of Tokyo and cluster machines in Nano-micro structure science and engineering, University of Hyogo.

---

[1] M. Z. Hasan and C. L. Kane, Rev. Mod. Phys. **82**, 3045 (2010).

[2] X. -L. Qi and S. C. Zhang, Rev. Mod. Phys. **83**, 1057 (2011).

[3] F. D. M. Haldane, Phys. Lett. A **93**, 464 (1983); Phys. Rev. Lett. **50**, 1153 (1983).

[4] J. P. Renard, M. Verdaguer, L. P. Regnault, W. A. C. Erkelens, J. Rossat-Mignod and W. G. Stirling, Europhys. Lett. **3**, 945 (1987).

[5] M. Hagiwara, K. Katsumata, Ian Affleck, B. I. Halperin, and J. P. Renard, Phys. Rev. Lett. **65**, 3181 (1990).

[6] I. Affleck, T. Kennedy, E. H. Lieb, and H. Tasaki, Phys. Rev. Lett. **59**, 799 (1987); Commun. Math. Phys. **115**, 447 (1987).

[7] M. den Nijs and K. Rommelse, Phys. Rev. B **40**, 4709 (1989).

[8] F. Pollmann, A. M. Turner, E. Berg, and M. Oshikawa, Phys. Rev. B **81**, 064439 (2010).

[9] Z.-C. Gu and X.-G. Wen, Phys. Rev. B **80**, 155131 (2009).

[10] T. Hirano, H. Katsura, and Y. Hatsugai, Phys. Rev. B **77**, 094431 (2008).

[11] A. P. Schnyder, S. Ryu, A. Furusaki, and A. W. W. Ludwig, Phys. Rev. B **78**, 195125 (2008).

[12] S. Ryu, A. P. Schnyder, A. Furusaki and A. W. W. Ludwig, New. J. Phys. **12**, 065010 (2010).

[13] A. Kitaev, AIP Conf. Proc. **1134**, 22 (2009).

[14] T. Kennedy, E. H. Lieb, and H. Tasaki. J. Stat. Phys. **53**, 383 (1988).

[15] N. V. Prokof'ev, B. V. Svistunov, and I. S. Tupitsyn, Sov. Phys. JETP **87**, 310 (1998).

[16] O. F. Syljuåsen and A. W. Sandvik, Phys. Rev. E **66**, 046701 (2002).

[17] Y. Kato, T. Suzuki, and N. Kawashima, Phys. Rev. E **75**, 066703 (2007).

[18] M. Matsumoto, C. Yasuda, S. Todo, and H. Takayama, Phys. Rev. B **65**, 014407 (2001).

[19] S.Wenzel and W. Janke, Phys. Rev. B **79**, 014410 (2009).

[20] J. Lou, A. W. Sandvik, and N. Kawashima, Phys. Rev. B **80**, 180414 (2009).

[21] Effective theories for the Néel-dimer phase transitions have been proposed, for example, in A. Tanaka and X. Hu, Phys. Rev. Lett. **95**, 036402 (2005).

[22] See, for example, T. Giamarchi, *Quantum Physics in One Dimension* (Oxford University Press, New York, 2004).

[23] L. Shekhtman, O. Entin-Wohlman, and A. Aharony, Phys. Rev. Lett. **69**, 836 (1992).

[24] See, for example, Appendix A of Ref. 8.

[25] J. des Cloizeaux, Jacques and J. J. Pearson, Phys. Rev. **128**, 2131 (1962).